

Supplemental information

**Molecular reorganization in bulk bottlebrush polymers: direct observation via nanoscale
imaging**

Nikolay Borodinov¹, Alex Belianinov^{1,2}, Dongsook Chang¹, Jan-Michael Carrillo¹, Matthew J. Burch^{1,2}, Yüewen Xu³, Kunlun Hong¹, Anton V. Ievlev^{1,2}, Bobby G. Sumpter¹, and Olga S. Ovchinnikova^{1,2,*}

¹Center for Nanophase Materials Science, Oak Ridge National Laboratory, Oak Ridge,
TN 37831

²Institute for Functional Imaging of Materials, Oak Ridge National Laboratory, Oak
Ridge, TN 37831

³Kimberly-Clark Corporation, Irving, TX 75038

* Author to whom correspondence should be addressed.

Olga S. Ovchinnikova

Center for Nanophase Materials Sciences

Oak Ridge National Laboratory

1 Bethel Valley Rd

Oak Ridge TN, 37831-6493

ovchinnikovo@ornl.gov

Notice: This manuscript has been authored by UT-Battelle, LLC, under Contract No. DE-AC0500OR22725 with the U.S. Department of Energy. The United States Government retains and the publisher, by accepting the article for publication, acknowledges that the United States Government retains a non-exclusive, paid-up, irrevocable, world-wide license to publish or reproduce the published form of this manuscript, or allow others to do so, for the United States Government purposes. The Department of Energy will provide public access to these results of federally sponsored research in accordance with the DOE Public Access Plan (<http://energy.gov/downloads/doe-public-access-plan>).

Section S.1: Scheme of bottlebrush under investigation

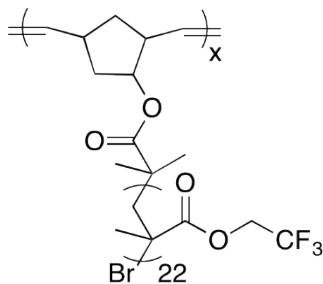


Figure S.1. Structure of the bottlebrush polymer used in the study.

Section S.2 Coarse-Grained Molecular Dynamics Simulations Method

Coarse-grained molecular dynamics simulations of thin films composed of bottlebrush molecules were performed using the LAMMPS¹⁻² molecular dynamics simulation package. Bottlebrush molecules consisting of connected Lennard-Jones (LJ) beads that have a main chain (backbone) and each backbone bead is connected to a shorter side chain. The LJ beads of the bottlebrush molecules, (with size σ and mass m),³ have non-bonded pairwise interaction potential that is described by a shifted and truncated Lennard-Jones potential,

$$U_{LJ} = \begin{cases} 4\epsilon_{LJ} \left[\left(\frac{\sigma}{r_{ij}} \right)^{12} - \left(\frac{\sigma}{r_{ij}} \right)^6 - \left(\frac{\sigma}{r_{cut}} \right)^{12} + \left(\frac{\sigma}{r_{cut}} \right)^6 \right] & r_{ij} \leq r_{cut} \\ 0 & r_{ij} > r_{cut} \end{cases} \quad (S1)$$

Here, r_{ij} is the distance between the i^{th} and j^{th} beads, σ is the bead diameter, r_{cut} is the cutoff distance and ϵ_{LJ} is the potential well depth in units of $k_B T$ or thermal energy. The bonds linking the side chain and backbone beads are described by the finite extensible nonlinear elastic (FENE) bond,

$$U_{FENE} = -\frac{1}{2} k_{bond} R_o^2 \ln \left[1 - \left(\frac{r}{R_o} \right)^2 \right] + 4k_B T \left[\left(\frac{\sigma}{r} \right)^{12} - \left(\frac{\sigma}{r} \right)^6 \right] + k_B T \quad (S2)$$

where $k_B T$ is the thermal energy, $k_{bond} = 30 k_B T / \sigma^2$ is the spring constant, $R_o = 1.5\sigma$ is the maximum extent of the bond, and r is the distance between two bonded beads.⁴ The first term is

attractive and extends to the maximum length of the bond, R_0 , while the second term, which is repulsive has a cutoff of $2^{1/6}\sigma$ corresponding to the minimum of the Lennard-Jones potential.

The initial configuration of the simulation box was prepared by arranging 108 bottlebrush molecules with backbone and side chain degrees of polymerization, $n = 80$ and $m = 10$, respectively, in a square lattice. The film thickness was set to $h=20\sigma$ by gradually compressing the simulation box in the z direction. While, the x and y dimensions, $L_x=L_y=L=77.07\sigma$, were adjusted such that the total bead number density, ρ , is $0.8 \sigma^{-3}$. This compression process proceeds up to a time interval of $5 \times 10^3 \tau$. (where τ is the reduced time unit $\tau = \sigma(m_i/k_B T)^{1/2}$, and m_i is the mass of a LJ bead.) Here, the system was under periodic boundary conditions in both x and y directions, and in the z direction, repulsive LJ walls ($U_{\text{wall}}=4k_B T[(\sigma/z_w)^{12}-(\sigma/z_w)^6]$, where z_w is the z distance of a bead from a wall and $U_{\text{wall}}=0$ if $z_w>2^{1/6}\sigma$) were applied in both top and bottom edges of the simulation box forming a thin film. After the compression process, to further relax the conformation of the bottlebrush molecules in the thin film, another $10^4 \tau$ equilibration run was performed in the canonical (NVT) ensemble, where all bead interactions are repulsive (or have $\epsilon_{\text{LJ}}=k_B T$ and $r_{\text{cut}}=2^{1/6}\sigma$ as parameters in eq.S1. In this step as well as all other stages of the simulations, the temperature was maintained by coupling the system to the Langevin thermostat at a temperature of $T=\epsilon_{\text{LJ}}/k_B$, such that the motions of the beads are described by the equation of motion,

$$m_i \frac{d\vec{v}_i(t)}{dt} = \vec{F}_i(t) - \xi \vec{v}_i(t) + \vec{F}_i^R(t) \quad (\text{S3})$$

where $m_i = 1$ is the bead mass, $\vec{v}_i(t)$ is the bead velocity, and $\vec{F}_i(t)$ denotes the net deterministic force acting on the i^{th} bead. The stochastic force $\vec{F}_i^R(t)$ has a zero average value $\langle \vec{F}_i^R(t) \rangle = 0$ and δ -functional correlations $\langle \vec{F}_i^R(t) \vec{F}_i^R(t') \rangle = 6k_B T \xi \delta(t - t')$. The bead friction coefficient ξ was set to $\xi = 1/7 m/\tau$. The velocity-Verlet algorithm with a time step of $\Delta t = 0.01 \tau$ was used for integrating the equations of motion in eq.S4. After which, the bottom wall was replaced with a non-moving 4σ thick layer that consists of randomly arranged LJ beads, and having a layer number density of $1 \sigma^{-3}$.

Next, the non-bonded pairwise interaction parameters between LJ beads were selected to simulate molecular interactions between three components, i.e. backbone (bead type 1), side-chains (bead type 2), and substrate (bead type 3). The interaction parameters were set to be $\epsilon_{13} = 0.25 k_B T$, $\epsilon_{23} = 0.25 k_B T$, when $\epsilon_{11} = 2 k_B T$, $\epsilon_{22} = 2 k_B T$, $\epsilon_{12} = 2 k_B T$ and $\epsilon_{33} = 1 k_B T$. The Flory-Huggins interaction parameters (χ) were estimated based on the geometric mean equation,

$$\chi_{ij} = \frac{1}{k_B T} \left[\frac{\epsilon_{ii} + \epsilon_{jj}}{2} - \epsilon_{ij} \right] \quad (\text{S4})$$

to be $\chi_{12} = 0$, $\chi_{13} = 1.25$ and $\chi_{23} = 1.25$. This system represents fully compatible backbone and side chain monomers (i.e. minimal difference in their chemical composition) with substrate and surface that are both neutral.

With these parameters, the pairwise interactions of the bottlebrush molecules are slightly above the T_g of the Kremer-Grest bead-spring model, allowing for the chains in the film to further relax their conformations.⁵ In addition, the attractive interactions defined in the new set of ϵ of the production runs results in the decrease in thickness of the thin film, which decreased from 20σ to

around 15σ . The production simulations run proceeded for $2 \times 10^5 \tau$ with the last $10^5 \tau$ range of trajectory frames, taken at an interval of 50τ , is used for data analysis.

Section S.3: HIM micrograph of the unetched film.

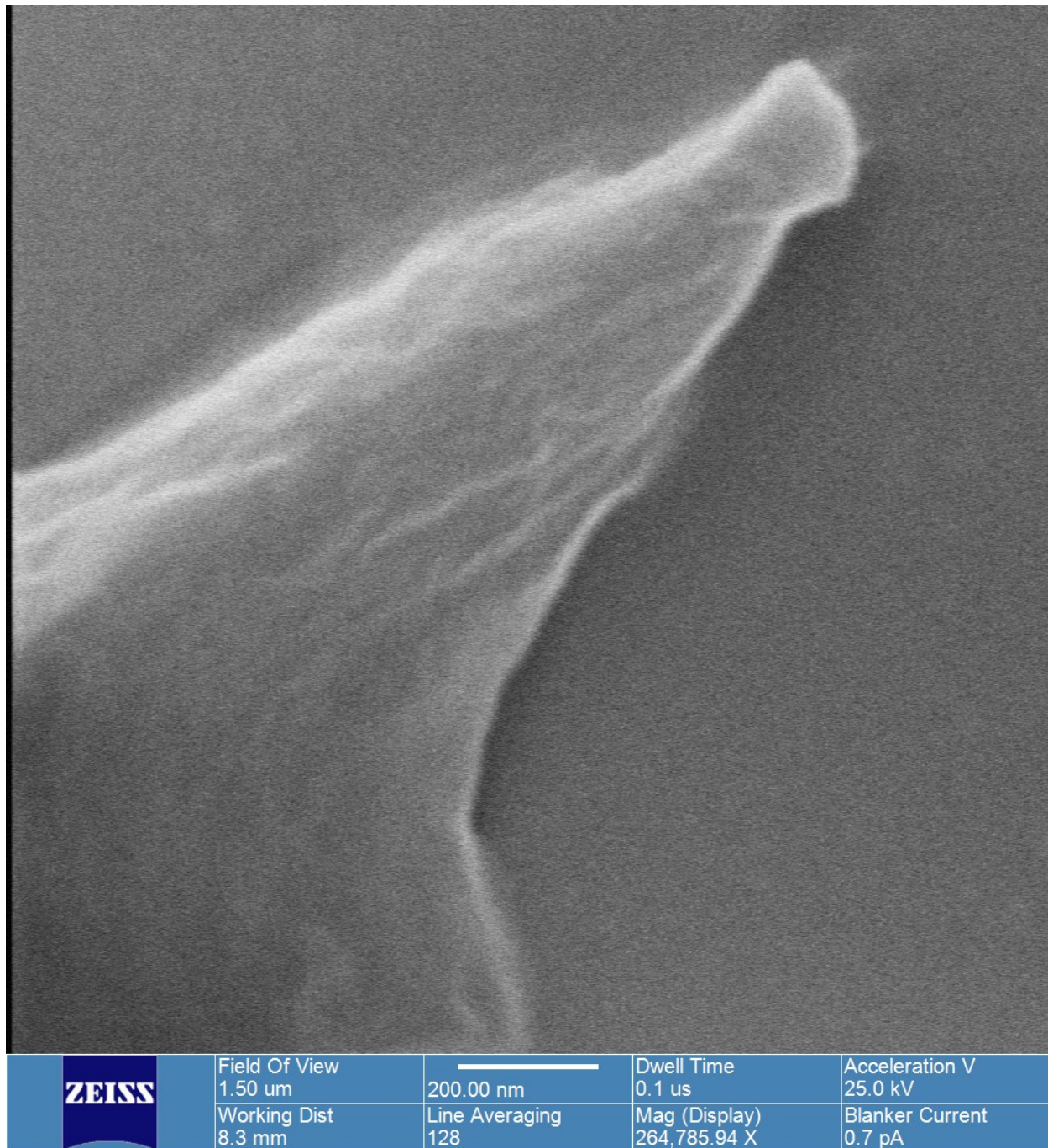


Figure S.2. HIM image of the unetched polymer bottlebrush film.

Section S.4: Height variation of plasma cleaned films

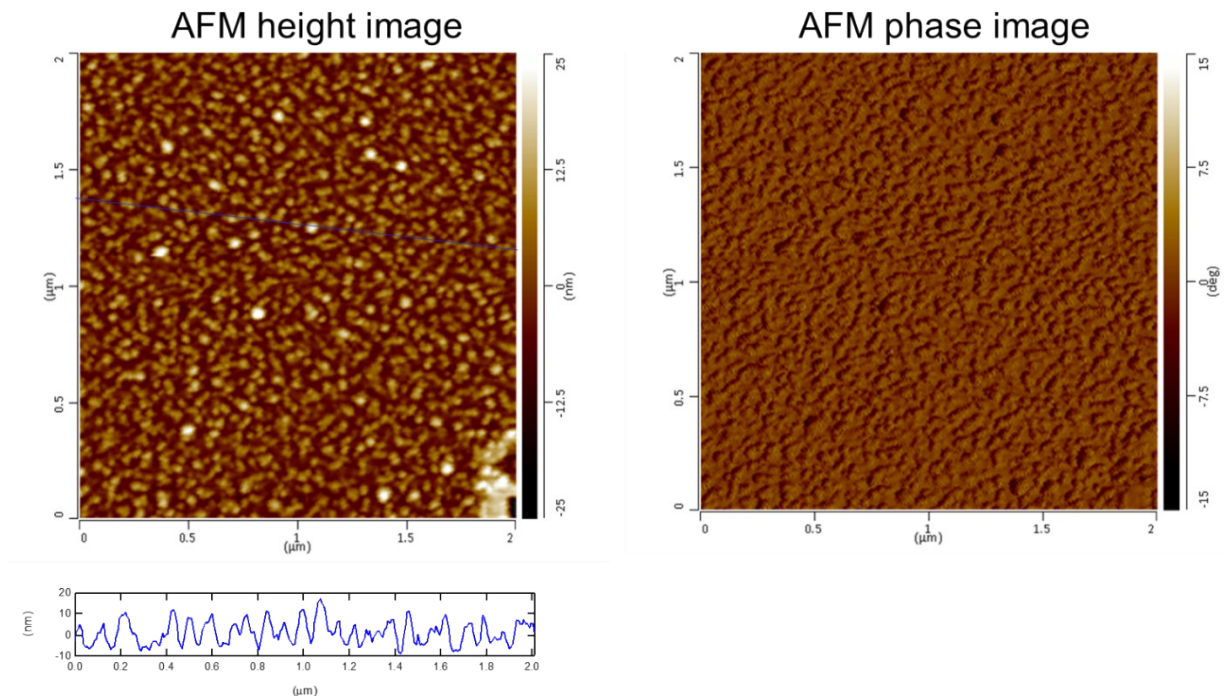


Figure S.3: AFM images of plasma cleaned bottlebrush films demonstrating the topography and phase images with a line profile across the center of the topographical image demonstrating the height variation across the films surface.

Section S.5: Pair distribution functions.

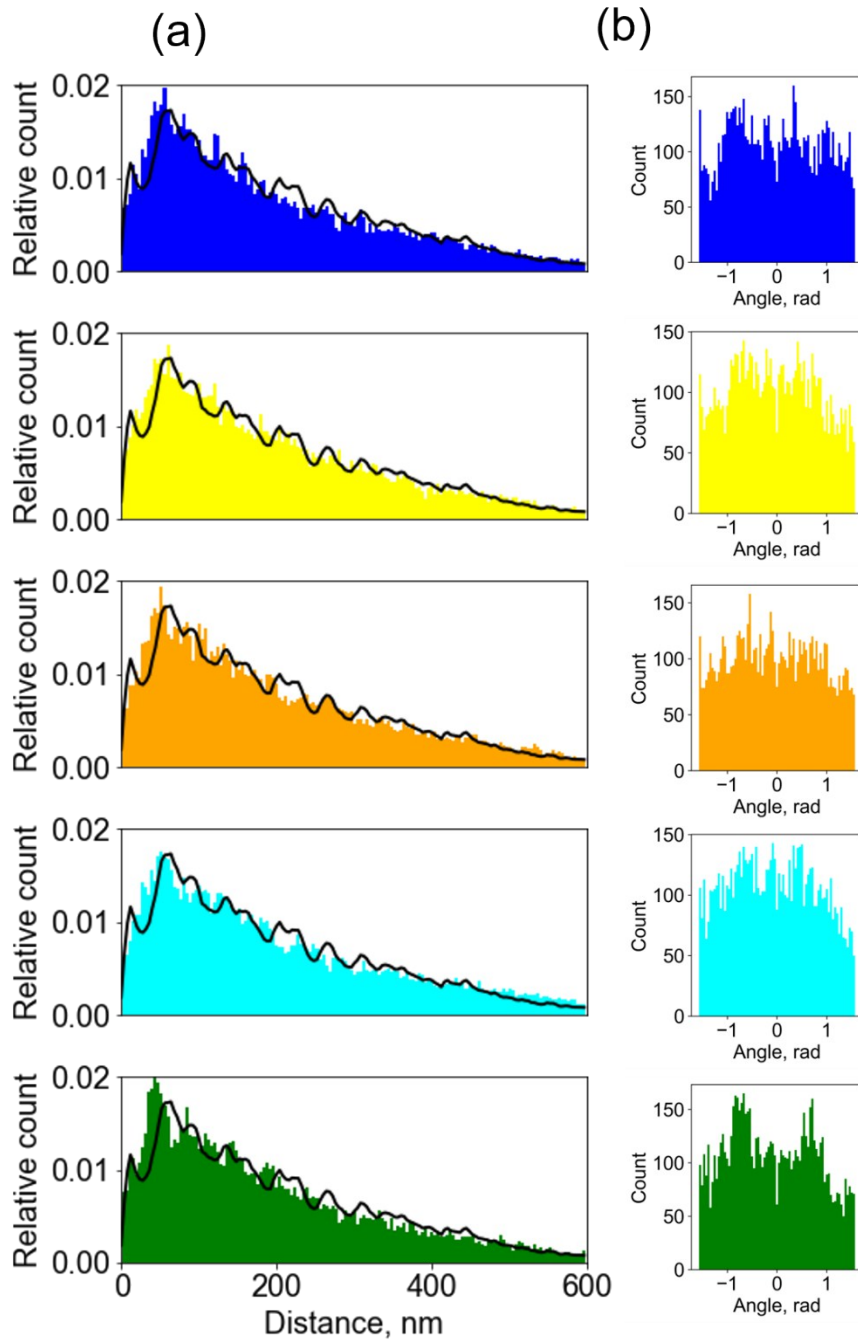


Figure S.4. Analysis of the five as-cast HIM micrographs: (a) intersegment distance calculation for those micrographs and (b) histogram of segment orientation for the corresponding images. Black line shows the distribution for the annealed film.

Section S.6: Pair distribution functions.

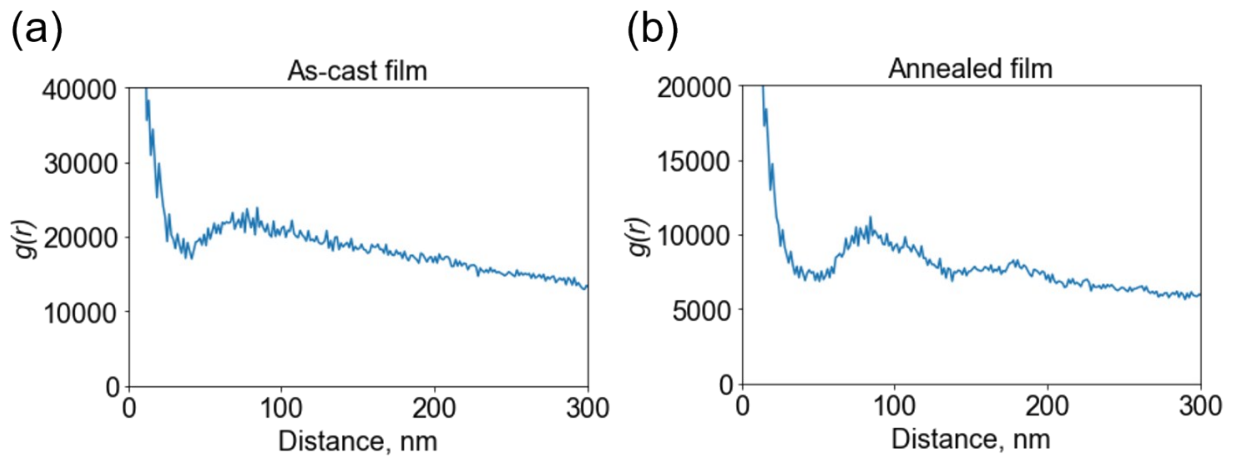


Figure S.5. Pair distribution functions $g(r)$ for the skeletonized micrograph of the (a) as-cast and (b) annealed films.

Section S.7 Orientational order parameter

$$S = \left\langle \frac{3\cos(\theta)^2 - 1}{2} \right\rangle \quad (\text{S5})$$

where θ is the angle between segment axis and the *local director*

Section S.8: Pixel-to-pixel spatial correlation function .

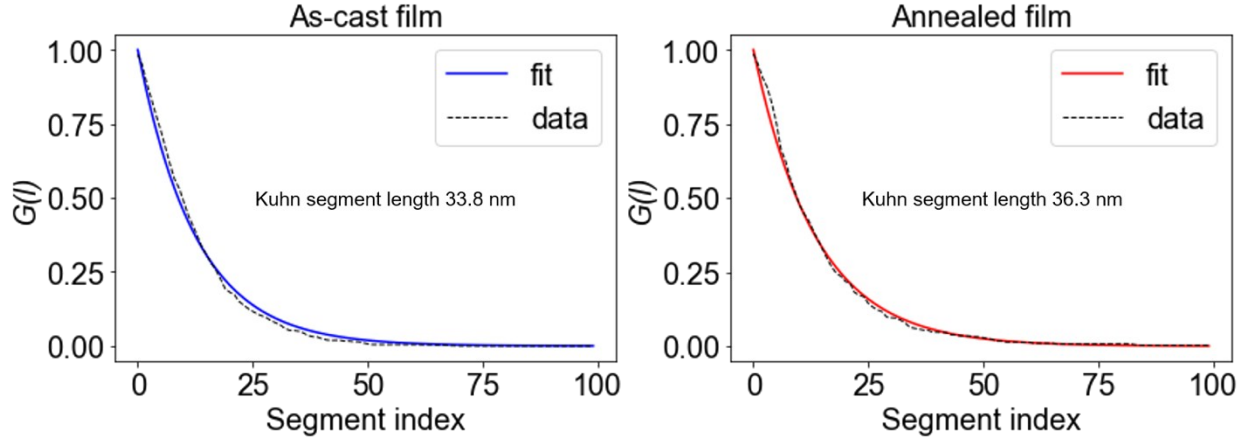


Figure S.6. Backbone bond-bond correlation function and Kuhn length for the (a) as-cast and (b) annealed films.

Pixel-to-pixel spatial correlation function approximate the bond-bond correlation.

Generally, the $G(l)$ is calculated as follows:

$$G(l) = \frac{1}{N_b - l} \sum_{i=1}^{N_b - l} \langle (\vec{n}_i \cdot \vec{n}_{i+l}) \rangle , \quad (S6)$$

where l is the segment index, N_b is the number of backbone bonds, \vec{n}_i is the i th unit vector parallel to the direction of the backbone bond. This data is fitted with the equation S7:

$$G(l) = (1 - \alpha)e^{-\frac{|l|}{\lambda_1}} + \alpha , \quad (S7)$$

Kuhn length (b_K) is then calculated as follows:

$$b_K \approx b((1 - \alpha)h(\lambda_1) + \alpha h(\lambda_2)) , \quad (S8)$$

Where b is pixel size and

$$h(\lambda) = \frac{1 + \alpha}{1 - \alpha} , \quad (S8)$$

In our case, one exponent is sufficient for the fitting for both as-cast and annealed images.

References:

- (1) Brown, W. M.; Wang, P.; Plimpton, S. J.; Tharrington, A. N. Implementing molecular dynamics on hybrid high performance computers—short range forces. *Computer Physics Communications* **2011**, *182* (4), 898-911.
- (2) Plimpton, S. Fast parallel algorithms for short-range molecular dynamics. *Journal of computational physics* **1995**, *117* (1), 1-19.
- (3) Carrillo, J.-M. Y.; Sumpter, B. G. Structure and dynamics of confined flexible and unentangled polymer melts in highly adsorbing cylindrical pores. *J. Chem. Phys.* **2014**, *141* (7), 074904.
- (4) Kremer, K.; Grest, G. S. Dynamics of entangled linear polymer melts: A molecular-dynamics simulation. *The Journal of Chemical Physics* **1990**, *92* (8), 5057-5086.
- (5) Tsige, M.; Lorenz, C. D.; Stevens, M. J. Role of network connectivity on the mechanical properties of highly cross-linked polymers. *Macromolecules* **2004**, *37* (22), 8466-8472.